Journal of Nuclear Materials 543 (2021) 152541

Contents lists available at ScienceDirect

Journal of Nuclear Materials

journal homepage: www.elsevier.com/locate/jnucmat

Short communication

Short communication: Spark plasma sintering as an innovative process for nuclear fuel plate manufacturing

Julien Havette[a,b], Xavière Iltis[a], Hervé Palancher[a], Olivier Fiquet[a], Mathieu Pasturel[b,*]

[a] CEA, DES, IRESNE, DEC, Cadarache F-13108, Saint-Paul-Lez-Durance, France
[b] Univ Rennes, CNRS, Institut des Sciences Chimiques de Rennes – UMR6226, F-35042 Rennes, France

ARTICLE INFO

Article history:
Received 22 July 2020
Revised 17 September 2020
Accepted 18 September 2020
Available online 22 September 2020

Keywords:
Materials testing reactors (MTR)
U_3Si_2
Spark plasma sintering (SPS)
Manufacturing process
Fuel plate

ABSTRACT

In this paper, we propose an alternative process based on spark plasma sintering for the manufacture of nuclear fuel plates for research reactors. This process presents significant flexibility to control manufacturing parameters such as fuel meat geometry and porosity according to the designer specifications. Furthermore, it allows to increase uranium loading up to 7.3 g_U cm^{-3}, exceeding the current requirements for high performance MTRs. With this process neither dogbone, fishtail nor sharp particles penetrating the cladding are observed. The potentialities of this approach are illustrated with the manufacturing of a high loaded (5.6 g_U cm^{-3}) U_3Si_2/Al mini-plate.

Material Testing Reactors (MTRs) are mostly used to study materials under irradiation and to produce radioisotopes for medical and industrial applications. The driver fuel of most MTRs is made of fuel plates in which powdered fissile material is dispersed in an aluminium matrix to constitute a fuel meat cladded with aluminium alloy plates.

In the 1980's, due to nuclear proliferation issues related to the use of High Enriched Uranium (HEU, >20% ^{235}U), it has been decided to convert MTRs to Low Enriched Uranium (LEU, <20% ^{235}U). With HEU fuels, the low uranium density UAl_x material (a mixture of different uranium aluminides) was often used [1]. In order to keep the same reactor performances using LEU fuels, new materials with higher uranium density have been developed. The most promising ones are γU(Mo) [2] and U_3Si_2 [1,3,4]. These fuel candidates are currently under qualification for their use in high performance MTRs [5], U_3Si_2/Al fuels being already qualified for low and medium power MTRs [4].

The fuel plates - typically about 1.3 mm thick, 70-100 cm long and 7 cm large - used in these reactors are manufactured by mixing fissile particles, sieved to reach a maximum diameter of 125 µm, with aluminium powder with a 44 µm max granulometry [4]. The mixed powders are then pressed to obtain a tough fuel meat, which is then encased in a frame and cladded by plates of aluminium alloy (AG3 or AlFeNi in most cases). Then, the edges of the plate are welded and this assembly is hot rolled (about 8 times) and cold rolled (2-3 times) [4]. The rolling steps of the manufacturing process aim at reaching the required plate thickness and ensuring cohesion between the different elements. For a long time, this manufacturing process has been successfully applied to γU(Mo)/Al and U_3Si_2/Al fuel plates (the latter qualified up to 4.8 g_U cm^{-3}). This process known as picture-frame (Fig. 1a) is worldwide considered as the industrial reference [6]. However some intrinsic limitations can be listed [7]: (i) dogboning which corresponds to an increase of the thickness of the meat at the edge of the plate, (ii) fish tails induced by differences in mechanical behaviour between the cladding and the meat, (iii) porosities caused by particles fragmentation during rolling which cannot be filled by aluminium deformation especially during cold rolling, (iv) sharp particles penetrating the cladding.

In this communication, an alternative process using spark plasma sintering (SPS) is proposed to overcome some of these limitations and to facilitate the manufacturing of plates with higher uranium loading.

SPS attracts strong interest because of its ability to obtain materials with fine microstructures [8,9]. It consists in fitting the powder or green compact to be sintered in an electrically conductive matrix, applying a uniaxial force and flowing a high intensity electrical current to induce a high speed consolidation. The main advantage of this technique is the short sintering time thanks to (i) its high achievable heating and cooling rates (100 to 1000 K min^{-1}) and (ii) local overheating (and hypothetically sparks) between the powder particles in the case of electrical conducting materials, promoting diffusion mechanisms and enhancing the

* Corresponding author.
E-mail address: mathieu.pasturel@univ-rennes1.fr (M. Pasturel).

https://doi.org/10.1016/j.jnucmat.2020.152541
0022-3115/

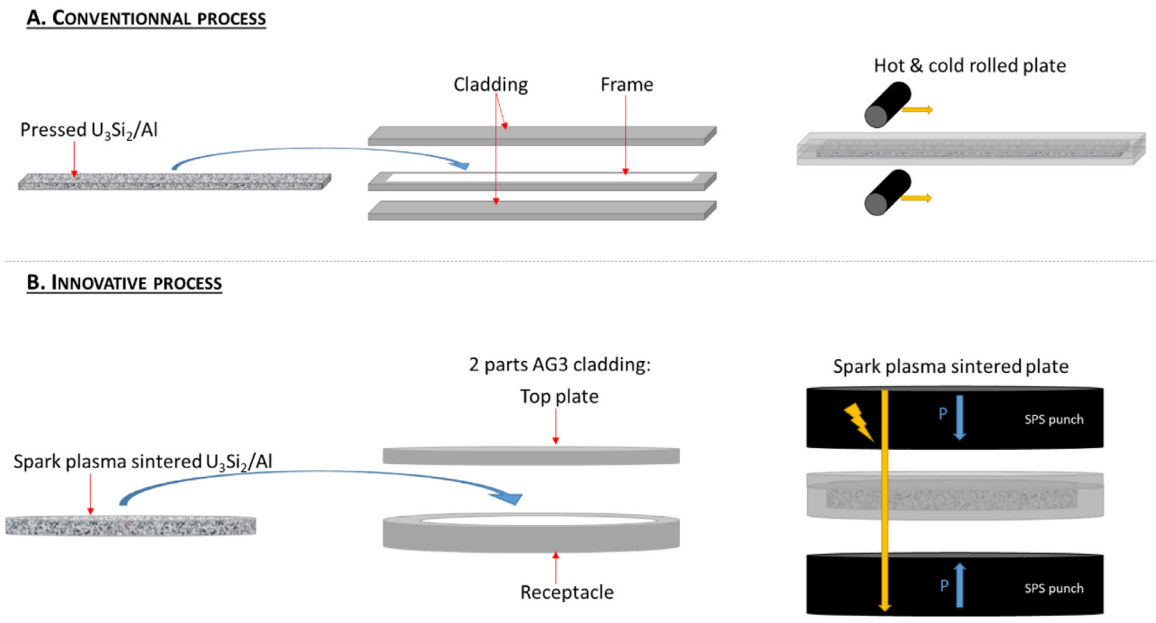

Fig. 1. Schematic representation of (A) the picture-frame technique and (B) the innovative process for preparation of U_3Si_2/Al nuclear fuel plates.

densification over grain growth. It has been successfully applied to U_3Si_2 powder to obtain pellets with fine microstructures, as part of the Accident Tolerant Fuel initiative, at temperatures between 1073 and 1573 K and dwell times between 3 and 20 minutes [10–13].

In this study, we applied SPS to a U_3Si_2/Al composite and showed that it could constitute a valid alternative to the pressing and rolling steps currently used for producing MTRs fuel plates.

For this purpose, U_3Si_2 particles provided by Framatome CERCA [14] were mixed with aluminium powder. An AG3 cladding was used for these experiments, comprising two elements (Fig. 1b): a receptacle (equivalent to the combination of plate and frame from the picture-frame process) and a top-plate. This cladding device was chosen to facilitate its machining and the round geometry of the plate for these preliminary experiments was imposed by the available sintering device.

The SPS machine we used was a HP-D-10 from FCT System GmbH (Germany). Die and punches are made in graphite for pressures up to 76 MPa and in tungsten carbide for higher pressures, with diameters between 10 and 40 mm. Both were coated with a graphite foil in order to facilitate demoulding. Sintering processes were performed under primary vacuum atmosphere with heating and cooling rates of 100 K min^{-1}.

The first step of this study focused on the preparation of the U_3Si_2/Al fuel meat alone while the second on the preparation of an entire fuel plate (fuel meat with AG3 cladding).

Densities of the sintered fuel meats were determined by helium pycnometry and Archimedes method. Fuel meats were polished to be characterized by X-ray diffraction (XRD) with a Bragg-Brentano θ-2θ Bruker D8 Advance diffractometer using monochromatized copper radiation (Cu $K_{\alpha 1}$, λ=1.5406 Å). Then fuel meats and plates were cut using a diamond wire saw and cross sections were polished for scanning electron microscopy (SEM) observations performed using a FEI Nova Nano SEM 450. The microscope is equipped with an Oxford Instruments SDD energy dispersive spectrometer (EDS) with an active surface of 80 mm^2. Working distance was set to 8 mm for a 15 kV high voltage.

The first phase of development focused on the fuel meat elaboration in order to define the optimized values for the sintering temperature, pressure and dwell time. With SPS, raw U_3Si_2 powders start to sinter at a temperature of 1073 K [11], *i.e.* above the melting point of aluminium (933 K). In the case of an U_3Si_2 + Al mixture, interaction between both components has to be avoided. For a maximum dwell time of 10 minutes, the sintering temperature must then be kept below 873 K [15–17]. This implies that during the SPS process of the fuel meat, densification mechanisms will mainly concern aluminium particles. About 300 mg of mixed powders with a 50%/50% volume ratio were put into a 10 mm diameter matrix for sintering, leading to about 0.5 mm thick fuel meats. In the case of a fully dense disc, the uranium loading would then be 5.6 g_U cm^{-3}. Upon characterization, particular attention was paid to the spatial distribution of fissile particles within the meat, the final density and the absence of interaction between U_3Si_2 and Al.

When the applied pressure was too high (> 150 MPa), part of the powder was expelled at the periphery of the matrix. Conversely, when using a too low pressure (or temperature), the weak resulting discs were difficult to handle due to their poor densification and significant porosity (Fig. 2a). With moderate temperature (800 K) and pressure (76 MPa), the sintered discs were tough enough and easily handled. Fig. 2b presents a SEM micrograph of a disc sintered in these conditions, with a 5 minutes dwell time. No interaction between U_3Si_2 and Al is noticed. This observation is confirmed by the XRD pattern acquired on the fuel meat surface, where only U_3Si_2 and Al phases are indexed (Fig. 3a). In the case of higher temperature (850 K for 5 minutes), an interaction between U_3Si_2 and the Al matrix occurs and leads to the formation of a few µm thick $U(Al,Si)_3$ (25at.% U, 15at.% Si and 60at.% Al according to EDS quantification) interaction layer around U_3Si_2 particles (Fig. 2c and 3b).

Open porosity (valued at approximately 3%, measured by Archimedes density) was only observed on the surface of the pellets and is attributed to roughness effects. The majority of this surface open porosity will be filled by the cladding during sintering while the deepest open porosity will be sealed by the cladding, leading to a slight increase of closed porosity.

According to pycnometry measurements (Fig. 4), all densities of sintered discs at 800 K – 76 MPa are greater than 97%, meaning that less than 3 vol.% of closed porosity is present before cladding. Few porosities (around 10 µm) are observed (contoured in red in Fig. 2b), mainly where U_3Si_2 particles are touching each other, confirming the absence of U_3Si_2 diffusion at this moderate tempera-

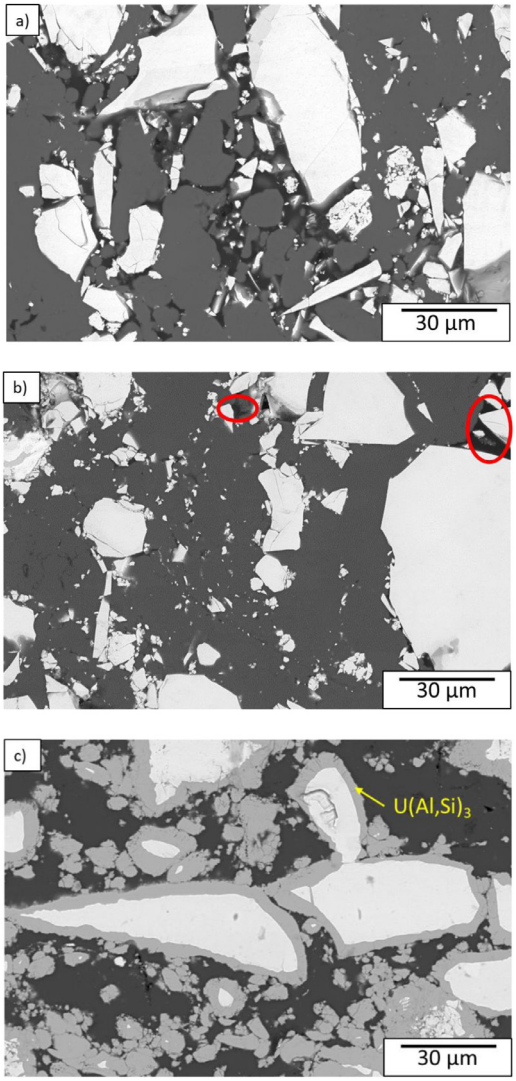

Fig. 2. Backscattered electron SEM images of U_3Si_2 particles (white) dispersed in Al matrix (dark grey) after spark plasma sintering at (a) 600 K, (b) 800 K and (c) 850 K, for 5 minutes under a pressure of 76 MPa. Some porosities between U_3Si_2 particles in (b) are highlighted by red circles. The $U(Al,Si)_3$ interaction layer in panel (c) appears in light grey.

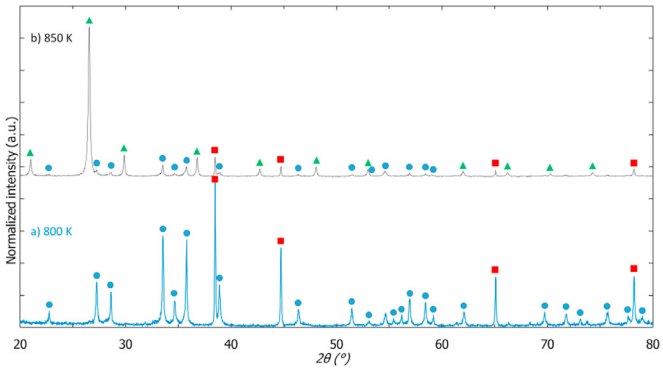

Fig. 3. X-ray diffraction patterns acquired on the surface of an U_3Si_2+Al fuel meat sintered at 76 MPa, with a dwell time of 5 minutes and an uranium loading of 5.6 g_U cm^{-3} at (a) 800 K and (b) 850 K. The diffraction peaks are indexed with ● U_3Si_2, ■ Al and ▲ $U(Al,Si)_3$ diffraction peaks.

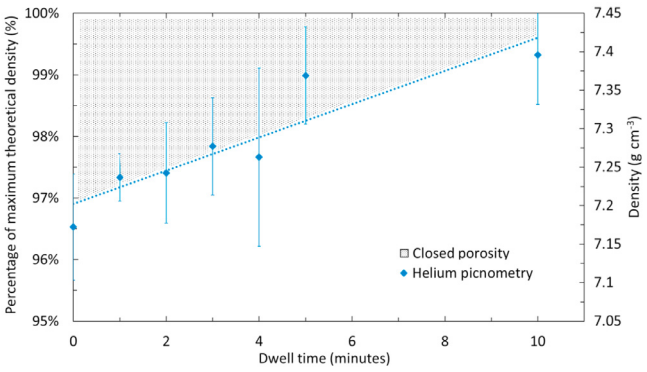

Fig. 4. He-pycnometry density (right axis) and its equivalent percentage of the maximum theoretical density (7.45 g cm^{-3} for a uranium loading of 5.6 g_U cm^{-3}, left axis) of U_3Si_2+Al fuel meats prepared by SPS, as a function of dwell time at 800 K - 76 MPa.

ture. This porosity ratio is low for such uranium loading (5.6 g_U cm^{-3}) and can be easily adapted to the designer's specifications by modifying temperature and/or dwell time (Fig. 4). This is a significant advantage over the conventional pressing process. It is important to note that a sintering dwell longer than 20 minutes at 800 K under 76 MPa leads to an interaction between U_3Si_2 and Al matrix.

This step of development was first applied to 10 mm diameter discs and secondly, with the same efficiency, on larger discs up to 40 mm diameter. This corresponds to the maximum diameter enabling to reach 76 MPa pressure with our SPS equipment. Our study focused on 0.5 mm thick fuel meat as it is the standard geometry used in fuel plates. On top of that, we applied the same process to fuel meats up to 2 mm thick. These experiments showed the same efficiency in terms of particle distribution and density, proving that this method would enable to easily adjust the fuel meat thickness.

The second step of this study consisted in manufacturing reduced scale fuel plates with an AG3 cladding. The home-designed cladding parts were first wiped with acetone and then etched with 10 wt.% sodium hydroxide solution and with a 40 wt.% nitric acid solution in order to achieve a good bonding between the different parts of the fuel plate by removing any oxidation layer or organic compounds from the Al-alloy surface [7]. The sintered fuel meat was placed inside the receptacle and covered by an AG3 plate (Fig. 1b). The different parts were then assembled by SPS in order to (i) create a strong cohesion between the AG3 cladding and the fuel meat and (ii) weld the two cladding parts together. This SPS process was applied to a 35 mm diameter fuel meat and 40 mm diameter receptacle resulting in a fuel plate of 40 mm diameter, using 76 MPa pressure, 775 K temperature and 3 minutes dwell time.

Particular attention was paid to the cohesion between the fuel meat and the cladding, the control of the fuel meat geometry (especially at the fuel plate edges) and the interface geometry.

Fig. 5a corresponds to 57 stitched SEM images of the cross section of the sintered fuel plate. The interface between the fuel meat and cladding is quite flat and no sharp particle penetrates into the cladding. The cladding thickness all along the plate section is virtually constant (not shown here), meaning that it will not be necessary to oversize it to guarantee the fuel safety. However, the outer surface of the fuel plate in contact with the punch has some surface roughness and is not perfectly flat. This point needs further improvement but could be easily solved by using flatter polished punches.

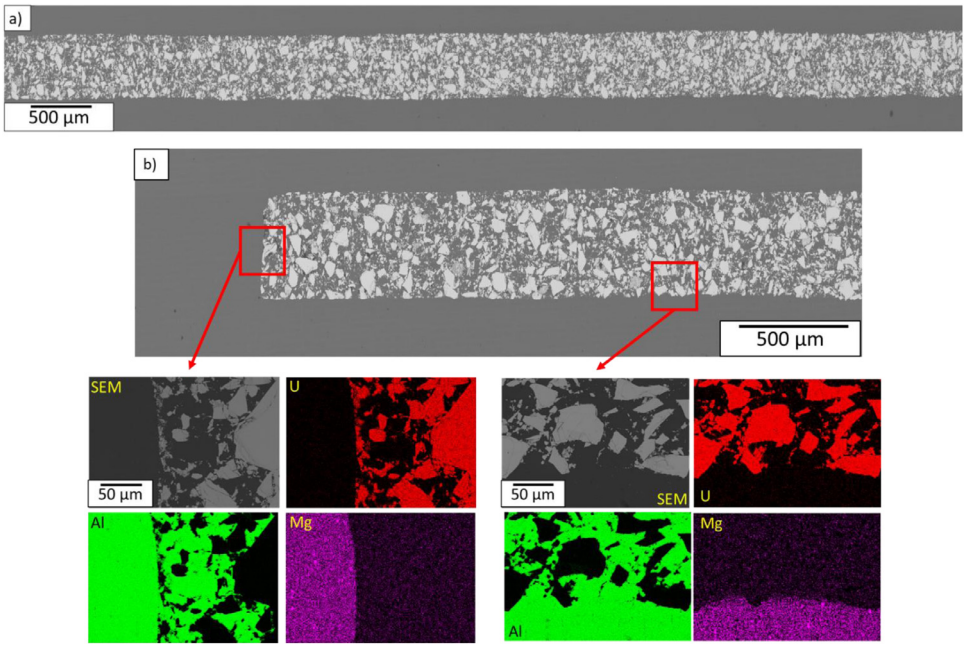

Fig. 5. (a) Stitched backscattered electron SEM images of a cross section of a U_3Si_2-based fuel plate manufactured by SPS, (b) Backscattered electron SEM images of the extremity of the plate and EDS X-ray maps acquired in areas boxed in red.

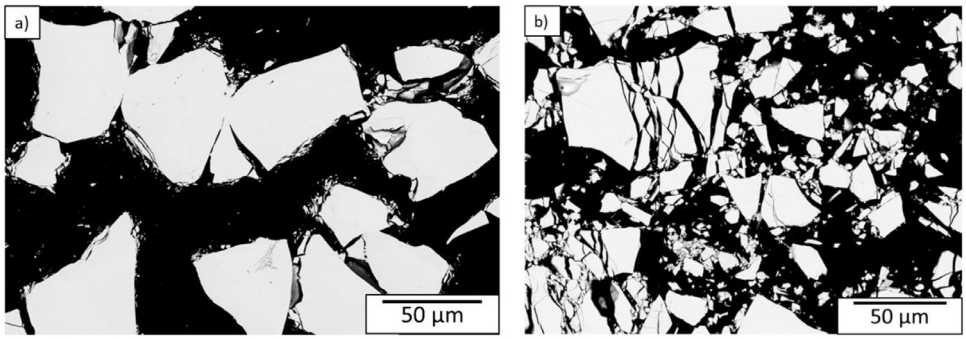

Fig. 6. Backscattered electron SEM images of fuel plates obtained (a) by SPS and (b) by rolling (taken from [3]). The aluminium matrix, porosities and cracks are shown in black and U_3Si_2 particles in white.

Thanks to this process, the geometry of the fuel meat is well controlled. Indeed, neither fish tail nor dogbone are observed at the extremities (Fig. 5b). Furthermore, a good cohesion between the fuel meat and the cladding is obtained, as illustrated by the EDS maps shown in Fig. 5b. Indeed, the continuity of Al between the fuel meat matrix and the cladding, revealed by the Al map, evidences the perfect bonding between the two parts. The cladding limit is clearly visible on the Mg map (AG3 contains around 3 wt.% Mg). It also confirms that the majority of open porosities present at the surface of the meat pellet are filled by the cladding.

The comparison of SEM images of the fuel plate sections obtained by SPS (Fig. 6a) and rolling (SHARE-type plate [18],Fig. 6b) clearly evidences that the first method generates much less U_3Si_2 particle fragmentation than the standard process. This fragmentation is the main cause of internal porosities within the final fuel plate, according to Durazzo *et al.* [7]. This means that the final characteristics (porosity and geometry) of the fuel plate can be set at the stage of the fuel meat manufacturing and controlled along the whole SPS process.

In this study, we demonstrate that the SPS has the potential of being an efficient manufacturing process for U_3Si_2/Al fuel plates of small dimension (40 mm diameter). Improvement is still needed but this technique presents many advantages: it allows an accurate control of the fuel meat geometry (neither dogbone nor fishtail), a decreased final porosity and less particles fragmentation.

Further work will focus on mechanical behaviour determination. In particular, three points bending tests will be performed to compare SPS-processed fuel plates with those fabricated with the standard picture-frame technique. These experiments will verify if the SPS-manufactured fuel plates may endure the shape deformation required for the fuel assembly. Microstructural characteristics of the rolled and sintered aluminium matrix will also be studied. Improvement of the cladding flatness and roughness will be targeted in further experiments.

In preliminary experiments, we observe that it is possible to increase the U_3Si_2/Al ratio up to 65 vol.% U_3Si_2 (*i.e.* 7.3 g_U cm^{-3}) without significant increase of the porosity level (which remained between 4 and 10 % depending on the dwell duration). In other words, with this process, loading limitations would probably not come from the manufacturing process but from the in-pile behaviour.

Currently and to the best of the authors knowledge, SPS furnaces can manufacture objects with maximum dimensions of a few tens of cm only [19], rather far from actual fuel plates dimensions. Up-scaling of the SPS process should be envisaged and motivates further developments.

Declaration of Competing Interest

The authors declare that they have no known competing financial interests or personal relationships that could have appeared to influence the work reported in this paper.

CRediT authorship contribution statement

Julien Havette: Conceptualization, Investigation, Methodology, Writing - original draft. **Xavière Iltis:** Project administration, Writing - review & editing, Supervision. **Hervé Palancher:** Funding acquisition, Writing - review & editing, Supervision. **Olivier Fiquet:** Project administration, Writing - review & editing, Supervision. **Mathieu Pasturel:** Conceptualization, Methodology, Writing - review & editing, Supervision.

Acknowledgements

Framatome-CERCA (Romans, France) is gratefully acknowledged for supplying the U_3Si_2 powder used in this study.

References

[1] Y.S. Kim, Uranium intermetallic fuels (U–Al, U–Si, U–Mo), Compr. Nucl. Mater. (2012) 391–422.
[2] S. Van den berghe, P. Lemoine, Review of 15 years of high-density low enriched umo dispersion fuel development for research reactors in Europe, Nucl. Eng. Technol. 46 (2014) 125–146, doi:10.5516/NET.07.2014.703.
[3] J. Havette, X. Iltis, H. Palancher, D. Drouan, O. Fiquet, E. Castelier, M Pasturel, From arc-melted ingot to MTR fuel plate: a SEM/EBSD microstructural study of U_3Si_2, J. Nucl. Mater. 537 (2020) 152224, doi:10.1016/j.jnucmat.2020.152224.
[4] Nuclear Regulatory Commission, Washington, DC (USA)Office of Nuclear Reactor Regulation *Safety Evaluation Report Related to the Evaluation of Low-Enriched Uranium Silicide-Aluminum Dispersion Fuel for Use in Non-Power Reactors*, 1988.
[5] S. Valance, H. Breitkreutz, Y. Calzavara, M. Hrehor, F. Huet, J. Jaroszewicz, H. Palancher, S. Van den Berghe, The H2020 European Project LEU-FOREVER: LEU Fuels for Medium and High Power Research Reactors in Europe, 2018 München, Germany.
[6] M.X. Milagre, U. Donatus, N.V. Mogili, C.S.C. Machado, J.V.S. Araujo, R.E. Klumpp, S.M.C. Fernandes, J.A.B. de Souza, I. Costa, Effects of picture frame technique (PFT) on the corrosion behavior of 6061 aluminum alloy, J. Nucl. Mater. (2020) 152320, doi:10.1016/j.jnucmat.2020.152320.
[7] M. Durazzo, E. Vieira, E.F. Urano de Carvalho, H.G. Riella, Evolution of fuel plate parameters during deformation in rolling, J. Nucl. Mater. 490 (2017) 197–210, doi:10.1016/j.jnucmat.2017.04.018.
[8] Saheb, N.; Iqbal, Z.; Khalil, A.; Hakeem, A.S.; Al Aqeeli, N.; Laoui, T.; Al-Qutub, A.; Kirchner, R. Spark plasma sintering of metals and metal matrix nanocomposites: a review available online: https://www.hindawi.com/journals/jnm/2012/983470/ (accessed on Jul 6, 2020).
[9] R. Chaim, G. Chevallier, A. Weibel, C. Estournès, Grain growth during spark plasma and flash sintering of ceramic nanoparticles: a review, J. Mater. Sci. 53 (2018) 3087–3105, doi:10.1007/s10853-017-1761-7.
[10] A. Mohamad, Y. Ohishi, H. Muta, K. Kurosaki, S. Yamanaka, Thermal and mechanical properties of polycrystalline U_3Si_2 synthesized by spark plasma sintering, J. Nucl. Sci. Technol. 0 (2018) 1–10, doi:10.1080/00223131.2018.1480431.
[11] N Brisset, Etude physico-chimique et des propriétés électroniques de composés uranifères binaires et ternaires dans les systèmes U-Si-B et U-Pt-Si, PhD thesis, Université de Rennes 1 (2016). http://www.theses.fr/2016REN1S135/document.
[12] B. Gong, T. Yao, P. Lei, J. Harp, A.T. Nelson, J Lian, Spark plasma sintering (SPS) densified U_3Si_2 pellets: microstructure control and enhanced mechanical and oxidation properties, J. Alloys Compd. 825 (2020) 154022, doi:10.1016/j.jallcom.2020.154022.
[13] D.A. Lopes, A. Benarosch, S. Middleburgh, K.D. Johnson, Spark plasma sintering and microstructural analysis of pure and Mo doped U_3Si_2 pellets, J. Nucl. Mater. 496 (2017) 234–241, doi:10.1016/j.jnucmat.2017.09.037.
[14] J. Durand, B. Duban, Y. Lavastre, CERCA's 25 years Experience in U_3Si_2 Fuel Manufacturing 25th International Meeting on RERTR, 2003.
[15] Y.S. Kim, G.L. Hofman, Interdiffusion in U_3Si–Al, U_3Si_2–Al, and USi–Al dispersion fuels during irradiation, J. Nucl. Mater. 410 (2011) 1–9, doi:10.1016/j.jnucmat.2010.12.031.
[16] M. Mirandou, S. Aricó, R. Sanabria, S. Balart, D. Podestá, J. Fabro, Study of the interaction between U_3Si_2/Al in dispersion plates at the end of the fabrication process, Nucl. Technol. 199 (2017) 96–102, doi:10.1080/00295450.2017.1323534.
[17] J. Marín, J. Lisboa, J. Ureta, L. Olivares, H. Contreras, J.C. Chávez, Synthesis and clad interaction study of U_3Si_2 powders dispersed in an aluminum matrix, J. Nucl. Mater. 228 (1996) 61–67, doi:10.1016/0022-3115(95)00167-0.
[18] A. Leenaers, E. Koonen, Y. Parthoens, P. Lemoine, S. Van den Berghe, Post-irradiation examination of AlFeNi cladded U_3Si_2 fuel plates irradiated under severe conditions, J. Nucl. Mater. 375 (2008) 243–251, doi:10.1016/j.jnucmat.2008.01.013.
[19] C.F. Gutiérrez-González, M. Suarez, S. Pozhidaev, S. Rivera, P. Peretyagin, W. Solís, L.A. Díaz, A. Fernandez, R. Torrecillas, Effect of TiC addition on the mechanical behaviour of Al_2O_3–SiC whiskers composites obtained by SPS, J. Eur. Ceram. Soc. 36 (2016) 2149–2152, doi:10.1016/j.jeurceramsoc.2016.01.050.